Partial Differential Equations in Applied Mathematics 14 (2025) 101218

Contents lists available at ScienceDirect

Partial Differential Equations in Applied Mathematics

journal homepage: www.elsevier.com/locate/padiff

Mathematical modeling of lumpy skin disease: New perspectives and insights

Goutam Saha [a,b], Pabel Shahrear [c], Abrar Faiyaz [c], Amit Kumar Saha [a,*]

[a] Department of Mathematics, University of Dhaka, Dhaka 1000, Bangladesh
[b] Miyan Research Institute, International University of Business Agriculture and Technology, Uttara, Dhaka 1230, Bangladesh
[c] Department of Mathematics, Shahjalal University of Science and Technology, Sylhet 3114, Bangladesh

ARTICLE INFO

Keywords:
Lumpy skin disease
Cows, Flies, Transmission
Stability
Bifurcation

ABSTRACT

This research presents a new mathematical structure featuring two compartments representing cows and flies. It aims to comprehensively understand the dynamics of Lumpy Skin Disease (LSD), incorporating a temperature-dependent mortality rate for flies. We thoroughly examine the model to establish the presence of a positive solution that remains bounded. By evaluating the disease's contamination potential and inspecting the model's stability concerning both local and global equilibrium points—namely, disease-free and endemic—we calculate the reproduction number. Theoretical analysis shows that a stable disease free equilibrium co-exists with a stable endemic equilibrium whenever the basic reproduction number is less than one implying the possibility of having backward bifurcation. Numerical simulation also supports this. Furthermore, through sensitivity analysis, we explore how various model parameters affect the basic reproduction number. Our numerical investigations underscore the critical importance of regulating specific parameters, such as the disease-induced mortality rate of cows, the temperature-dependent mortality rate of flies, and the rate of transition from infected to recovered cows, in effectively managing the disease system. Numerical results also show that controlling flies population and spraying adulticide, LSD spread can be prevented.

1. Introduction

Lumpy skin disease, commonly referred to as LSD, was first identified in the city of Chittagong, Bangladesh, during March-April 2019. This initial observation marked the beginning of a concerning outbreak, as the highly contagious viral disease swiftly spread among cows across the entire country.[1] Being a skin disease, LSD possesses a remarkable capacity for rapid transmission and efficient contagion. The primary mode of transmission involves infected cows acting as carriers, where flies play a significant role in facilitating the spread of the disease. These insects become vectors by coming into contact with the infected cows and then transferring the pathogen to other susceptible individuals, thereby exacerbating the rapid expansion of the outbreak. While the outbreak in Bangladesh shed light on the devastating impact of LSD, it is worth noting that the disease has a long history dating back to its believed origin in Zambia, Africa, in 1929. During that time, the emergence of LSD in Zambia resulted in the unfortunate loss of numerous cows and led to the closure of several farms. Since then, the disease has continued to pose a threat, traversing geographical boundaries and making its presence felt in different parts of the world. One such notable occurrence was in 2013 when LSD surfaced in Turkey. This marked a significant turning point as the disease successfully made its way into Asia, setting the stage for further spread across the region.

Again, in 2023, an outbreak of lumpy disease, affecting cattle, emerged in Bangladesh and swiftly spread across the entire nation. It is believed that hundreds of thousands of cows have fallen victim to this ailment, leading to the devastating loss of thousands of lives within the bovine community. Unfortunately, despite the deployment of vaccines in an attempt to combat the disease, their effectiveness has been disappointingly limited, failing to adequately address the severity of the situation. Despite the government's swift response and the deployment of available vaccines, the battle against the lumpy disease in Bangladesh

Abbreviations: ANN, Artificial neural network; CFR, Case fatality rate; ELISA, Enzyme-linked immunosorbent assay; MaxEnt, Maximum entropy ecological niche modeling.

* Corresponding author.
E-mail addresses: gsahamath@du.ac.bd (G. Saha), shahrear-mat@sust.edu (P. Shahrear), chowdhuryabrarfaiyaz@gmail.com (A. Faiyaz), amit92.du@gmail.com (A.K. Saha).

https://doi.org/10.1016/j.padiff.2025.101218
Received 5 February 2025; Received in revised form 25 April 2025; Accepted 25 April 2025
Available online 30 April 2025

has proven to be an arduous one. Regrettably, the efficacy of the vaccines implemented has fallen short of expectations, rendering their impact insufficient in curbing the spread and severity of the disease. This unfortunate turn of events has left farmers, veterinarians, and policymakers grappling with the challenge of finding alternative strategies to safeguard the cattle population effectively.

Molla et al.[2] conducted a study in Ethiopia, employing an SIR mathematical model alongside statistical analysis to examine the transmission rate parameter of LSD. Their findings revealed an alarming initial transmission rate, primarily attributable to the absence of preventive measures. Consequently, the study recommends implementing early control measures to mitigate the spread of LSD. Ardestani and Mokhtari[3] examined the likelihood of LSD occurrence in western Iran by employing MaxEnt. They gathered data from 2012 to 2016 and determined that the presence of LSD is influenced by various weather elements, including low temperatures (-1 to 6 °C), moderate rainfall (140-160 mm), humidity, and cold conditions. Sarkar et al.[4] conducted an investigation into the LSD outbreaks in the Dinajpur district, Bangladesh, focusing on a cohort of 453 afflicted cattle, of which 186 were diagnosed as LSD-positive. Results indicate that the containment of LSD transmission can be effectively managed through the implementation of systematic vaccination protocols, robust disease control measures, diligent disinfection practices, and particular attention paid to the well-being of female cattle. Hasib et al.[5] conducted a cross-sectional inquiry to elucidate the occurrence of Lumpy Skin Disease (LSD) in firm animals within the region of Chittagong, Bangladesh during the year 2019. The investigation encompassed a sizable cohort of 3327 farm animals, among which 120 individuals were detected with LSD infection. Intriguingly, the results unveiled that the prevalence of LSD was notably elevated in hybrid and female livestock. Moreover, it was discerned that the inclusion of new animals into the farm environment represented a prominent risk factor for the transmission of this disease. Haque et al.[6] undertook a comprehensive survey-based investigation aimed at assessing the extant condition of LSD and its associated handling practices across several agrarian enterprises situated in the Natore district, Bangladesh. Spanning from June to December 2020, the data collection phase encompassed a meticulous examination of 34 animal farms, comprising a substantial population of 87 animals. Notably, their discerning analysis uncovered a conspicuous prevalence of LSD infection among female cattle, a trend that resonates with the congruent findings reported by Hasib et al.[5]. These congruent observations underscore the importance of gender-specific factors in the manifestation and spread of LSD among bovine populations in the region. Khalil et al.[7] conducted research on LSD epidemics in Barisal, Bangladesh. The data was gathered in 2019, encompassing a sample of 3630 livestock. The findings revealed that out of this population, 686 cattle tested positive for LSD. The study indicated that young cattle accounted for 24 % of the infected cases, while pregnant cattle represented 70 %, making them more susceptible to the disease compared to other animals. Pory et al.[8] orchestrated a cross-sectional investigation into the prevalence of LSD (Lumpy Skin Disease) outbreaks in veterinary hospitals in Sylhet, Bangladesh in 2020. The study involved a substantial sample of 2762 cattle, out of which 377 were identified as LSD-positive. The findings revealed a noteworthy surge in cases during the months of May and June 2020 constituting approximately 47 % and 49 % of the total incidence, respectively.

Chouhan et al.[9] conducted an extensive investigation aimed at comprehending the economic repercussions of LSD on cattle in Bangladesh. This survey centered on two specific districts, namely Mymensingh and Gaibandha. Data was meticulously gathered from October 2019 to June 2020, where a total of 1187 cattle were randomly selected for analysis, out of which 403 were identified as infected, and tragically, 13 died due to LSD-related consequences. The consequential impact of LSD on the economy of both districts was markedly substantial, resulting a loss of around 92 million USD. Issimov et al.[10] conducted a cross-sectional study aiming to investigate the risk factors associated with LSD. They utilized a questionnaire to collect data from 543 households in west Kazakhstan from January 2021 to July 2021. The research employed multivariate logistic regression analysis. They highlighted that the buying and selling of animals during LSD virus outbreaks contribute to the spread of the virus. They further emphasized the significance of farmer awareness and training to effectively manage and prevent future LSD outbreaks. Safavi[11] employed a machine learning technique to forecast the future occurrence of the LSD virus in cattle by considering the environmental conditions. The study found that when predicting the future incidence of the LSD virus in cattle, ANN exhibited superior performance compared to other algorithms. Uddin et al.[12] conducted an investigation into the incidence of LSD outbreaks across nine distinct regions in Bangladesh spanning from December 2019 to December 2020. The study revealed that out of the total 8215 cattle examined, 603 were found to be LSD-positive. Notably, Narsingdi exhibited the highest CFR at 1.51, followed closely by Kishoreganj at 1.38 and Rangpur at 1.36. Conversely, Naogaon exhibited the lowest CFR at 0.52, indicating a lower fatality rate in comparison to other districts.

In a recent study, Alfwzan et al.[13] devised a mathematical model that takes into account the interactions between cattle (Susceptible-Infected-Removal class), vectors (Susceptible-Infected class), and the environment. They made the assumption of a constant birth rate for both cattle and vectors. The results of their research suggest that implementing disinfection measures in the environment and minimizing the transmission between vectors and cattle could significantly aid in reducing the transmission of LSD. In a separate investigation, Butt et al.[14] presented a mathematical model that examined the effectiveness of a vaccination program as a control strategy for LSD. Their model incorporated susceptible-vaccination-exposed-infected-removal classes for cattle. The study revealed that implementing a vaccination strategy proved to be an effective approach in mitigating the spread of the LSD virus among cattle. Considering this finding in conjunction with the previous study by Alfwzan et al.[13] on different mathematical models, it becomes evident that combining strategies such as vaccination, disinfection, and reducing transmission between vectors and cattle holds promise for effectively managing and reducing the transmission of LSD. Moonchai et al.[15] created various mathematical models for analyzing the trend of LSD in Thailand during the period of 2021-2022. The mathematical models they proposed include the Lorentzian, Gaussian, Pearson-type VII, two-Lorentzian, two-Gaussian, two-Pearson-type VII, Richard's growth, Boltzmann sigmoidal, and Power-law growth models. Sthitmatee et al.[16] created an in-house-based ELISA test kit to identify the LSD virus. Their findings revealed that their test kit performed comparably to a commercially available ELISA test kit. To evaluate the efficacy of the ELISA test kit, they conducted this research on a sample size of 460 dairy cows. Sayed et al.[17] conducted an inquiry into the demographic determinants contributing to the occurrence of Lumpy Skin Disease (LSD) in the Barisal district of Bangladesh, spanning from January 2021 to June 2022. The study involved a substantial sample size of 2047 cattle that underwent LSD testing at various hospitals, with 44 of them testing positive for the disease. The findings revealed that certain factors, such as specific breeds, female gender, and advanced age of cattle, exhibited a more pronounced prevalence rate compared to other variables. Remarkably, the highest incidence of LSD was recorded in June 2022, peaking at 13.39 %. More recent research is available in.[18-20]

According to the available literature and research in the field, most of the studies are based on statistical analysis. There are only two research works based on mathematical modeling: one focuses solely on the cattle population with a vaccination strategy, and the other focuses on cattle and vector populations with limited compartments for each population. Considering this research gap, we considered SEIR (cows)-SI (flies) mathematical model for LSD that comprehensively captures the intricacies of their interactions and spread dynamics. Therefore, this study undertakes the task of developing a SEIR-SI model that encompasses all potential transmission routes responsible for the spread of LSD. The

critical transmission pathways considered include vector transmission and direct transmission between cattle and flies. By considering both vector and direct transmission, the SEIR-SI model opens up new avenues for investigating the various factors influencing the disease's spread and control. Consequently, this research aims to contribute valuable insights into managing LSD outbreaks and implementing effective prevention strategies.

In the following, we will present first present the novel mathematical model for LSD disease, then disease-free equilibrium (DFE) and endemic equilibrium points within epidemiological frameworks. Our analysis will incorporate several pivotal components, including the determination of the reproduction number at DFE, the positivity of solutions, the behavior of local asymptotic stability at DFE, details of Lyapunov functions, and sensitivity analysis. Furthermore, to enhance our explanation, we will present some numerical findings that will explain the practical outcomes of the discussed theoretical constructs.

2. Mathematical model

This study employs a compartmentalized approach to model the dynamics of LSD infection, which considers both cattle and vector populations. The cattle population is categorized into four distinct compartments: susceptible cattle (S_C), exposed cattle (E_C), infected cattle (I_C), and recovered cattle (R_C). On the other hand, the vector population, which includes flies, is divided into two compartments: susceptible vector (S_M) and infected vector (I_M).

Hence, total population of cows is, $N_C = S_C + E_C + I_C + R_C$,and total flies population is$N_v = S_M + I_M$.

Schematic diagram of the LSD model is presented in Fig. 1. By integrating these compartments we can portray the evolutionary dynamics of LSD infection through the following model. Also, Table 1 describes the model parameters whereas Table 2 displays the numerical values of the model parameters.

We have considered the following assumptions during model formulation:

Birth related recruitment has not been considered and the recruitment rates for both cow population and fly population are considered constant.
The model assumes a direct transmission pathway between cows and flies but cow-to-cow transmission has not been considered.
It is assumed that exposed cows can't transmit infection.
Re-infection of recovered cows has not been considered.
Temperature dependent death of flies has been taken into account.

Cow (C) – Flies (M)

$$\frac{dS_C}{dt} = \Lambda_1 - \frac{\beta_1}{N_C} S_C I_M - \mu_1 S_C \tag{1a}$$

$$\frac{dE_C}{dt} = \frac{\beta_1}{N_C} S_C I_M - \alpha_1 E_C - \mu_1 E_C \tag{1b}$$

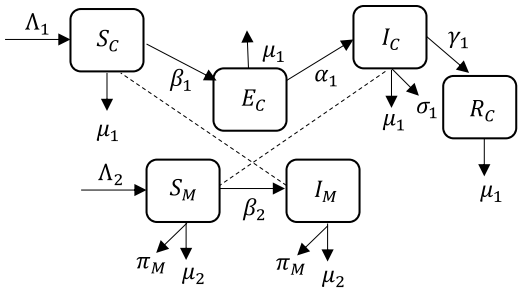

Fig. 1. Schematic diagram of the LSD model.

Table 1
Parameters used in the model and their descriptions.

Parameters	Description
Λ_1,Λ_2	Recruitment rate of cows and flies, respectively
β_1	Rate of transmission from infected flies to susceptible cows
β_2	Rate of transmission from infected cows to susceptible flies
μ_1,μ_2	Natural death rate of cows and flies, respectively
π_M	Temperature-dependent death rate of flies
α_1	Rate of transfer from exposed class to infected class for cows
σ_1	Disease-induced death rate of cows
γ_1	Rate of transfer from infected class to recovered class for cows

Table 2
Initial values for different compartments and different parameter values.

Initial conditions & Parameters	Values	Ref.	Initial conditions & Parameters	Values	Ref.
S_C	10000	-	Λ_1	100	Assumed
E_C	50	-	Λ_2	20000	Assumed
I_C	1	-	β_1	0.1	Assumed
R_C	0	-	β_2	0.2	Assumed
S_M	100000	-	α_1	0.2	Estimated
I_M	100	-	γ_1	0.008	[13]
μ_1	0.0002	Estimated	σ_1	0.008	[13]
μ_2	0.066	Estimated	π_M	0.20	Assumed

$$\frac{dI_C}{dt} = \alpha_1 E_C - \gamma_1 I_C - \sigma_1 I_C - \mu_1 I_C \tag{1c}$$

$$\frac{dR_C}{dt} = \gamma_1 I_C - \mu_1 R_C \tag{1d}$$

$$\frac{dS_M}{dt} = \Lambda_2 - \frac{\beta_2}{N_C} S_M I_C - \mu_2 S_M - \pi_M S_M \tag{1e}$$

$$\frac{dI_M}{dt} = \frac{\beta_2}{N_C} S_M I_C - \mu_2 I_M - \pi_M I_M \tag{1f}$$

with initial condition

$$(S_C(0), E_C(0), I_C(0), R_C(0), S_M(0), I_M(0)) = (S_{C0}, E_{C0}, I_{C0}, R_{C0}, S_{M0}, I_{M0}) \tag{1g}$$

and

$$S_{C0}, E_{C0}, I_{C0}, R_{C0}, S_{M0}, I_{M0} \geq 0. \tag{1h}$$

In this model$\Lambda_1$and$\Lambda_2$represent the constant recruitment rate of cows and flies, respectively, where$\mu_1$and$\mu_2$are natural death rates of cows and flies, respectively. The average lifespan of cow is approximately 15 to 20 years. Assuming 15 years in this study, the numerical value of natural mortality rate is approximately$\mu_1 = 1/(15 \times 365) = 0.0002\text{day}^{-1}$. Similarly, average life expectancy of fly is approximately 15-30 days and hence considering 15 days for this study, the natural mortality rate is approximately$\mu_2 = 1/15 = 0.066\text{day}^{-1}$. Here,$\beta_1and\beta_2$represents the effective contact rate for LSD transmission. According to literature, warm temperatures help proliferate the fly populations, but extreme temperatures can have the opposite effect, reducing population growth rates and causing mortality. So, in this study, we have considered temperature-dependent death rate of flies (π_M). The incubation period for LSD is 4 to 14 days. During numerical simulation, we have assumed 5 days as incubation period and hence $\alpha_1 = 1/5 = 0.2$represents the transferred rate from exposed to infected class. $\sigma_1$and$\gamma_1$represent disease-related death rate and recovery rate of cows, respectively.

3. Theoretical outcomes

Theorem 1 (*Positivity of solutions*): The solution

$$\mathscr{K}(t) = (S_C(t), E_C(t), I_C(t), R_C(t), S_M(t), I_M(t)) \tag{2}$$

of the Lumpy skin disease (LSD) model (1) with $\mathscr{K}(0) \geq 0$ is non-negative for $t > 0$.

Proof: Let us consider Eq. (1a):

$$\frac{dS_C}{dt} = \Lambda_1 - (\mathscr{X} + \mu_1)\, S_C \text{ where } \mathscr{X} = \frac{\beta_1}{N_C} I_M \tag{3}$$

Solving, we get,

$$\frac{d}{dt}\left[S_C(t)\exp\left\{\mu_1 t + \int_0^t \mathscr{X}(u)du\right\}\right] = \Lambda_1 \exp\left\{\mu_1 t + \int_0^t \mathscr{X}(u)du\right\} \tag{4}$$

Integrating, we get

$$\begin{aligned} &S_C(t)\exp\left\{\mu_1 t + \int_0^t \mathscr{X}(u)du\right\} - S_C(0) \\ &= \int_0^t \Lambda_1 \exp\left\{\mu_1 v + \int_0^v \mathscr{X}(w)dw\right\}dv \end{aligned} \tag{5}$$

It follows that

$$\begin{aligned} S_C(t) = {} & S_C(0)\exp\left\{ -\left(\mu_1 t + \int_0^t \mathscr{X}(u)du\right)\right\} + \exp\left\{ \right. \\ & \left. -\left(\mu_1 t + \int_0^t \mathscr{X}(u)du\right)\right\} \times \int_0^t \Lambda_1 \exp\left\{\mu_1 v + \int_0^v \mathscr{X}(w)dw\right\}dv \\ & > 0 \end{aligned} \tag{6}$$

Similarly, we can show that

$$E_C(t) > 0, \quad I_C(t) > 0, \quad R_C(t) > 0, \quad S_M(t) > 0, \quad I_M(t) > 0$$

Therefore,

$\mathscr{K}(t) \geq 0$ for all $t > 0$.

Theorem 2: The set Ddefined as

$$D = \{(S_C,\ E_C,\ I_C, R_C,\ S_M,\ I_M) \in C : N_C \leq \Lambda_1 / \mu_1,\ N_M \leq \Lambda_2/(\mu_2 + \pi_M\ \} \tag{7}$$

is positively invariant and attracting.

Proof: Consider the differential equation for N_C

$$\frac{dN_C}{dt} = \Lambda_1 - \mu_1 N_C - \sigma_1 I_C \tag{8}$$

$$\frac{dN_C}{dt} \leq \Lambda_1 - \mu_1 N_C = \mu_1\left(\frac{\Lambda_1}{\mu_1} - N_C\right) \tag{9}$$

The above differential inequality can be solved to get

$$N_C(t) \leq \frac{\Lambda_1}{\mu_1} - \left(\frac{\Lambda_1}{\mu_1} - N_C(0)\right)e^{-\mu_1 t} \tag{10}$$

Therefore, we see that even if N_C was initially outside$D$, i.e., if$N_C(0) \geq \Lambda_1/\mu_1$, we will eventually have that$N_C \leq \Lambda_1/\mu_1$. This can be easily seen by taking the limit $t \to \infty$ in the inequality. We can do a similar analysis for N_M starting with its differential equation

$$\frac{dN_M}{dt} = \Lambda_2 - (\mu_2 + \pi_M)N_M \tag{11a}$$

$$\frac{dN_M}{dt} \leq \Lambda_2 - K_3 N_M = K_3\left(\frac{\Lambda_2}{K_3} - N_M\right), \text{ where } K_3 = \mu_2 + \pi_M \tag{11b}$$

$$N_M(t) \leq \frac{\Lambda_2}{K_3} - \left(\frac{\Lambda_2}{K_3} - N_M(0)\right)e^{-\mu_2 t} \tag{11c}$$

Therefore, we see that no matter what the initial conditions are, we will either have $N_c \to \Lambda_1/\mu_1$ and $N_M \to \Lambda_2/K_3$ asymptotically or at some future time we will have $N_C \leq \Lambda_1/\mu_1$ and$N_M \leq \Lambda_2/K_3$. So, the set D is positively invariant, bounded and attracting.

4. Equilibrium points and reproduction number

We determine the Disease-Free Equilibrium (DFE) point by equating the steady-state equations of the model (1) to zero. In this scenario, we assume the absence of the virus in the cattle, meaning infection does not persist in the population. Conversely, for the Endemic Equilibrium (EE), we presume the virus remains within the cattle population.

Disease-free equilibrium (DFE):

$$\mathscr{D}_{\mathscr{E}} = (S_C, 0,\ 0,\ 0, S_M, 0) \tag{12a}$$

Solving the following equations, we get

$$\Lambda_1 - \mu_1 S_C = 0 \tag{12b}$$

$$\Lambda_2 - \mu_2 S_M - \pi_M S_M = 0 \tag{12c}$$

$$\Rightarrow S_C = \frac{\Lambda_1}{\mu_1}, S_M = \frac{\Lambda_2}{K_3} \tag{12d}$$

Reproduction number for DFE:

The Reproduction number R_0 is calculated using the next-generation matrix technique. Essentially, it is the spectral radius of the product matrix $\mathscr{F}\mathscr{V}^{-1}$, where $\mathscr{F}$ represents the Jacobian of the rate of new infections and $\mathscr{V}$ represents the Jacobian of the rate of other translational terms in equations related to illness.[21]

$$\mathscr{F} = \begin{pmatrix} \frac{\beta_1}{N_C} S_C I_M \\ 0 \\ \frac{\beta_2}{N_C} S_M I_C \end{pmatrix} \tag{13a}$$

$$\mathscr{V} = \begin{pmatrix} K_1 E_C \\ -\alpha_1 E_C + K_2 I_C \\ K_3 I_M \end{pmatrix} \tag{13b}$$

where$K_1 = (\alpha_1 + \mu_1)$, $K_2 = (\gamma_1 + \sigma_1 + \mu_1)$,and$K_3 = \mu_2 + \pi_M$.

Then we have

$$\mathscr{F} = \begin{pmatrix} 0 & 0 & \frac{\beta_1}{N_C} S_C \\ 0 & 0 & 0 \\ 0 & \frac{\beta_2}{N_C} S_M & 0 \end{pmatrix} \tag{13c}$$

$$\mathscr{V} = \begin{pmatrix} K_1 & 0 & 0 \\ -\alpha_1 & K_2 & 0 \\ 0 & 0 & K_3 \end{pmatrix} \tag{13d}$$

Now,

$$\mathscr{V}^{-1} = \begin{pmatrix} \frac{1}{K_1} & 0 & 0 \\ \frac{\alpha_1}{K_1 K_2} & \frac{1}{K_2} & 0 \\ 0 & 0 & \frac{1}{K_3} \end{pmatrix} \tag{13e}$$

The next generation matrix is

$$\mathscr{F}\mathscr{V}^{-1} = \begin{pmatrix} 0 & 0 & \frac{\beta_1 S_C}{K_3 N_C} \\ 0 & 0 & 0 \\ \frac{\alpha_1\beta_2 S_M}{K_1 K_2 N_C} & \frac{\beta_2 S_M}{K_2 N_C} & 0 \end{pmatrix} \tag{14}$$

Eigenvalues of $\mathscr{F}\mathscr{V}^{-1}$ are

$$\lambda_1 = 0 \tag{15a}$$

$$\lambda_2 = -\frac{1}{N_C}\sqrt{\frac{\alpha_1\beta_1\beta_2 S_C S_M}{K_1 K_2 K_3}} \tag{15b}$$

$$\lambda_3 = \frac{1}{N_C}\sqrt{\frac{\alpha_1\beta_1\beta_2 S_C S_M}{K_1 K_2 K_3}} \tag{15c}$$

Hence,

$$R_0 = \frac{1}{K_3 N_C}\sqrt{\frac{\alpha_1\beta_1\beta_2\Lambda_1\Lambda_2}{\mu_1 K_1 K_2}} \tag{16}$$

Theorem 3: The disease free equilibrium (DFE) is locally asymptotically stable (LAS) if$R_0 < 1$.

Proof: At the DFE, i.e., at $\mathscr{D}_{\mathscr{E}} = \left(\frac{\Lambda_1}{\mu_1}, 0,\ 0,\ 0, \frac{\Lambda_2}{K_3}, 0\right)$ the Jacobian is as follows

$$J(\mathscr{D}_{\mathscr{E}}) = \begin{pmatrix} -\mu_1 & 0 & 0 & 0 & 0 & -P_1 \\ 0 & -K_1 & 0 & 0 & 0 & P_1 \\ 0 & \alpha_1 & -K_2 & 0 & 0 & 0 \\ 0 & 0 & \gamma_1 & -\mu_1 & 0 & 0 \\ 0 & 0 & -P_2 & 0 & -K_3 & 0 \\ 0 & 0 & P_2 & 0 & 0 & -K_3 \end{pmatrix} \tag{17}$$

where$P_1 = \frac{\beta_1}{N_c}\frac{\Lambda_1}{\mu_1}$, and $P_2 = \frac{\beta_2}{N_c}\frac{\Lambda_2}{K_3}$. For Eigenvalues, we have to solve the characteristics polynomial of six degree, i.e., $|J(\mathscr{D}_{\mathscr{E}}) - \lambda I| = 0$, which means

$$\begin{vmatrix} -\mu_1-\lambda & 0 & 0 & 0 & 0 & -P_1 \\ 0 & -K_1-\lambda & 0 & 0 & 0 & P_1 \\ 0 & \alpha_1 & -K_2-\lambda & 0 & 0 & 0 \\ 0 & 0 & \gamma_1 & -\mu_1-\lambda & 0 & 0 \\ 0 & 0 & -P_2 & 0 & -K_3-\lambda & 0 \\ 0 & 0 & P_2 & 0 & 0 & -K_3-\lambda \end{vmatrix} = 0 \tag{18}$$

After simplifications, we came up with this determinant

$$(-\mu_1-\lambda)(-\mu_1-\lambda)(-K_3-\lambda)\begin{vmatrix} -K_1-\lambda & 0 & P_1 \\ \alpha_1 & -K_2-\lambda & 0 \\ 0 & P_2 & -K_3-\lambda \end{vmatrix} = 0 \tag{19}$$

Characteristic polynomial is

$$(-\mu_1-\lambda)(-\mu_1-\lambda)(-K_3-\lambda)\left[\lambda^3 + B_1\lambda^2 + B_2\lambda + B_3\right] = 0 \tag{20}$$

Where,

$$B_1 = (K_1+K_2+K_3),\ B_2 = (K_1K_2+K_2K_3+K_3K_1),\ B_3 = K_1K_2K_3 - K_4,\ K_4 = \alpha_1 P_1 P_2.$$

Coefficients$B_1$and$B_2$are positive since$K_1 = (\alpha_1 + \mu_1)$and $K_2 = (\gamma_1 + \sigma_1 + \mu_1)$are positive. $K_3 = \mu_2 + \pi_M$is also positive. Finally, $K_4$is also positive as$P_1$and P_2 are positive. Therefore, based on Routh-Hurwitz stability criteria, we can conclude that all eigenvalues are negative if $B_3$is positive, that is, if the condition $K_1\ K_2\ K_3 > K_4$ holds. Hence, the DFE is locally asymptotically stable for $R_0 < 1$. When the condition $K_1\ K_2\ K_3 > K_4$ does not hold, then $R_0 > 1$ and the system will be unstable. This implies, LSD will persist.[28] Hence the theorem is proved.

Endemic equilibrium (EE):

$$\mathscr{E}_{\mathscr{E}} = \left(S_C^*, E_C^*,\ I_C^*,\ R_C^*, S_M^*, I_M^*\right) \tag{21a}$$

Let us set

$$\frac{dS_C}{dt} = \frac{dE_C}{dt} = \frac{dI_C}{dt} = \frac{dR_C}{dt} = \frac{dS_M}{dt} = \frac{dI_M}{dt} = 0 \tag{21b}$$

Then we have

$$\Lambda_1 - \frac{\beta_1}{N_C}S_C^* I_M^* - \mu_1 S_C^* = 0 \tag{22a}$$

$$\frac{\beta_1}{N_C}S_C^* I_M^* - \alpha_1 E_C^* - \mu_1 E_C^* = 0 \tag{22b}$$

$$\alpha_1 E_C^* - \gamma_1\ I_C^* - \sigma_1\ I_C^* - \mu_1\ I_C^* = 0 \tag{22c}$$

$$\gamma_1\ I_C^* - \mu_1 R_C^* = 0 \tag{22d}$$

$$\Lambda_2 - \frac{\beta_2}{N_C}S_M^*\ I_C^* - \mu_2 S_M^* - \pi_M S_M^* = 0 \tag{22e}$$

$$\frac{\beta_2}{N_C}S_M^*\ I_C^* - \mu_2 I_M^* - \pi_M I_M^* = 0 \tag{22f}$$

Adding the first four equations i.e., 22(a) to 22(d) gives

$$\Lambda_1 - \sigma_1\ I_C^* - \mu_1\left(S_C^* + E_C^* + I_C^* + R_C^*\right) = 0 \tag{22g}$$

Since $S_C^* + E_C^* + I_C^* + R_C^* = N_C^*$, we have

$$\Lambda_1 - \sigma_1\ I_C^* - \mu_1 N_C^* = 0 \tag{22h}$$

$$\Rightarrow N_C^* = \frac{\Lambda_1 - \sigma_1\ I_C^*}{\mu_1} \tag{22i}$$

Adding the last two equations i.e., 22(e) to 22(f) gives

$$\Lambda_2 - K_3\left(S_M^* + I_M^*\right) = 0 \tag{22j}$$

$$\Rightarrow N_M^* = \frac{\Lambda_2}{K_3} \tag{22k}$$

Then from Eq. 22(e), we get

$$S_M^* = \left(\frac{\Lambda_2\ \left[\Lambda_1 - \sigma_1\ I_C^*\right]}{K_3\Lambda_1 + \ \left[\beta_2\ \mu_1 - K_3\sigma_1\right]\ I_C^*}\right) \tag{22m}$$

Now, $S_M^* + I_M^* = N_M^*$ implies $I_M^* = N_M^* - S_M^*$. Then we get

$$I_M^* = \frac{\Lambda_2}{K_3} - \frac{\Lambda_2}{K_3}\frac{\left[\Lambda_1 - \sigma_1\ I_C^*\right]}{\left[\Lambda_1 - \sigma_1\ I_C^* + \frac{\beta_2\mu_1 I_C^*}{K_3}\right]} \tag{22n}$$

After simplification we find,

$$I_M^* = \frac{\beta_2\mu_1\Lambda_2 I_C^*}{K_3\beta_2\mu_1 I_C^* + (K_3)^2\left[\Lambda_1 - \sigma_1\ I_C^*\right]} \tag{22p}$$

$$\Rightarrow I_M^* = \frac{a\ I_C^*}{b - cI_C^*}, \tag{22q}$$

where $a = \beta_2\mu_1\Lambda_2$,$b = \Lambda_1(K_3)^2$ and $c = K_3(\beta_2\mu_1 - K_3\sigma_1)$.

Now rearranging 22(c) and 22(d) gives

$$E_C^* = \frac{K_2}{\alpha_1}I_C^*\ \&\ R_C^* = \frac{\gamma_1}{\mu_1}I_C^* \tag{22r}$$

Finally adding 22(a) and 22(b) gives

$$\Lambda_1 - \mu_1 S_C^* - K_1 E_C^* = 0. \tag{22s}$$

$$\Rightarrow S_C^* = \frac{\Lambda_1}{\mu_1} - \frac{K_1}{\mu_1} E_C^* \tag{22t}$$

Then from Eq. 22(b) we have

$$\beta_1 \left[\frac{\Lambda_1}{\mu_1} - \frac{K_1 K_2}{\alpha_1 \mu_1} I_C^*\right] \left[\frac{a\, I_C^*}{b - c I_C^*}\right] \left[\frac{\mu_1}{\Lambda_1 - \sigma_1\, I_C^*}\right] = \frac{K_1 K_2}{\alpha_1} I_C^* \tag{22u}$$

After laborious algebraic calculations on Eq. 22(u), we ultimately arrive at the following equation.

$$\chi_1 \left(I_C^*\right)^2 + \chi_2\, I_C^* + \chi_3 = 0, \tag{23a}$$

where

$$\chi_1 = \frac{K_1 K_2 \sigma_1}{\alpha_1 \Lambda_1} \tag{23b}$$

$$\chi_2 = \frac{K_1 K_2}{\alpha_1}\left[\frac{a\,\beta_1}{\Lambda_1} - \frac{b\,\sigma_1}{\Lambda_1} - c\right] = \frac{K_1 K_2 (K_3)^2}{\alpha_1}\left(R_0^2 - \frac{\beta_2 \mu_1}{K_3}\right) \tag{23c}$$

$$\chi_3 = \frac{K_1 K_2 b}{\alpha_1} - a\,\beta_1 = \frac{K_1 K_2 \Lambda_1 (K_3)^2}{\alpha_1}\left(1 - R_0^2\right) \tag{23d}$$

The number of endemic equilibria points depend on the number of positive real roots of this equation. The different cases are

a. No endemic equilibrium if:
i. $\chi_2 > 0$ and $\chi_3 > 0$, or
ii. $(\chi_2)^2 - 4\chi_1\chi_3 < 0$
b. One endemic equilibrium if:
i. $\chi_3 < 0$, or
ii. $\chi_2 < 0$, $\chi_3 > 0$ and $(\chi_2)^2 - 4\chi_1\chi_3 = 0$
c. Two endemic equilibria if $(\chi_2)^2 - 4\chi_1\chi_3 > 0$, $\chi_2 < 0$ and $\chi_3 > 0$

From the expressions of χ_1,χ_2 and χ_3 in terms of R_0, it can be shown that

$$\left(\frac{\alpha_1}{K_1 K_2 K_3^2}\right)^2 \left(\chi_2^2 - 4\chi_1\chi_3\right) = \left(R_0^2 - \frac{\beta_2\mu_1}{K_3}\right)^2 - 4\frac{\sigma_1}{K_3^2}\left(1 - R_0^2\right) \tag{24}$$

Let R_1 and R_2 be the solutions for the values of R_0 that satisfies the equation

$$\left(R_0^2 - \frac{\beta_2\mu_1}{K_3}\right)^2 - 4\frac{\sigma_1}{K_3^2}\left(1 - R_0^2\right) = 0 \tag{25}$$

provided$R_0 < 1$, and$R_1 < R_2$. Then the above three different cases can be written in terms of conditions on the basic reproduction number as

A. No endemic equilibrium if:
i. $\sqrt{\beta_2\mu_1/K_3} < R_0 < 1$, or
ii. $R_1 < R_0 < R_2$
B. One endemic equilibrium if:
i. $R_0 > 1$, or
ii. $R_0 < \min\left(1,\ \sqrt{\beta_2\mu_1/K_3}\right)$ and $R_0 = R_1$ or R_2
C. Two endemic equilibria if $R_0 < \min\left(1,\ \sqrt{\beta_2\mu_1/K_3}\right)$ and, either $R_0 < R_1$ or $R_0 > R_2$

Thus, as long as$R_0 > 1$, there will always be an endemic equilibrium point, but there may also be one or more endemic equilibrium points if$R_0 < 1$. Merely decreasing R_0 to less than unity is not sufficient. We must also decrease $\sqrt{\beta_2\mu_1/K_3}$ to less than unity, and keep R_0 between one and that value. Otherwise, we might have to decrease R_0 further until it becomes less thanR_2, if a positive value of R_2 exists. Therefore, it seems that the single most important parameter to control isK_3, which is the flies death rate. Allocating resources towards increasing the flies' death rate rather than attempting to lower their birth rate seems to be the most efficient strategy for epidemic eradication according to our model. This is illustrated in the Fig. 2.

Backward bifurcation analysis of the LSD model

Case (c) of the above discussion says that, we may have the possibility of having two endemic equilibrium whenever $R_0 < 1$and hence there may exist backward bifurcation phenomenon. Now using the Center Manifold Theory discussed in,[23] we will examine the existence of backward bifurcation. This will be done by using the changes of variable method. So, let $S_c = x_1$,$E_c = x_2$,$I_c = x_3$,$R_c = x_4$,$S_m = x_5$,and$I_m = x_6$.Hence in vector form the model (1) can be written as

$$\frac{dX}{dt} = \left(f_1, f_2, f_3, f_4, f_5, f_6\right)^T \tag{26}$$

where$X = (x_1, x_2, x_3, x_4, x_5, x_6)^T$ and then we have

$$\frac{dx_1}{dt} = f_1 = \Lambda_1 - \frac{\beta_1 x_6}{N_c} x_1 - \mu_1 x_1 \tag{27a}$$

$$\frac{dx_2}{dt} = f_2 = \frac{\beta_1 x_6}{N_c} x_1 - (\alpha_1 + \mu_1) x_2 \tag{27b}$$

$$\frac{dx_3}{dt} = f_3 = \alpha_1 x_2 - (\sigma_1 + \gamma_1 + \mu_1) x_3 \tag{27c}$$

$$\frac{dx_4}{dt} = f_4 = \gamma_1 x_3 - \mu_1 x_4 \tag{27d}$$

$$\frac{dx_5}{dt} = f_5 = \Lambda_2 - \frac{\beta_2 x_3}{N_c} x_5 - (\mu_2 + \pi_m) x_5 \tag{27e}$$

$$\frac{dx_6}{dt} = f_6 = \frac{\beta_2 x_3}{N_c} x_5 - (\mu_2 + \pi_m) x_6 \tag{27f}$$

The Jacobian of the system (27) is given by:

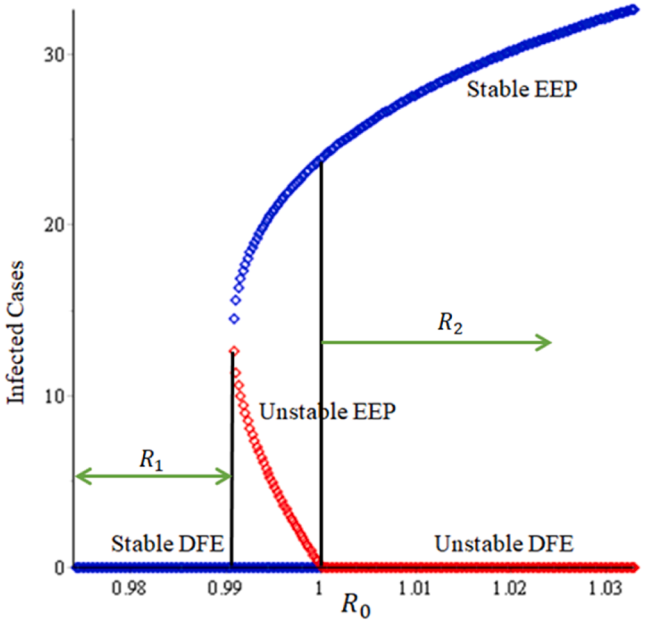

Fig. 2. Numerical simulation of the model (1) depicting the existence of backward bifurcation.

$$J(D_{\mathscr{E}}) = \begin{pmatrix} -\mu & 0 & 0 & 0 & 0 & -\beta_1 \\ 0 & -k_1 & 0 & 0 & 0 & \beta_1 \\ 0 & \alpha & -k_2 & 0 & 0 & 0 \\ 0 & 0 & \gamma & -\mu & 0 & 0 \\ 0 & 0 & -J_1 & 0 & -k_3 & 0 \\ 0 & 0 & J_1 & 0 & 0 & k_3 \end{pmatrix} \tag{28}$$

where

$$J_1 = \frac{\mu\ \beta_2\ \Lambda_2}{\Lambda_1(\pi_m + \mu_2)}$$

Now consider, $R_0 = 1$ and $\beta_1 = \beta_1^*$ is a bifurcation parameter. Thus we get,

$$\beta_1 = \beta_1^* = \frac{K_3^2 N_c^2 \mu_2 K_1 K_2}{\alpha_1 \beta_2 \Lambda_1 \Lambda_2} \tag{29}$$

The Jacobian $J(\mathscr{J}_{\mathscr{E}})$ of (27) with $\beta_1 = \beta_1^*$, denoted by $J_{\beta_1^*}$, has a simple zero eigenvalue (with all other eigenvalues having negative real part). Hence, the center manifold theory can be used to analyze the dynamics of the model (1).

Eigenvector of $J_{\beta_1^*} = J(\mathscr{J}_{\mathscr{E}})|_{\beta_1=\beta_1^*}$:

When$R_0 = 1$, the Jacobian ($\mathscr{J}_{\beta_1^*}$) of (27) has a right eigenvector given by

$W = (w_1, w_2, w_3, w_4, w_5, w_6)^T$where,

$$w_1 = -\frac{\beta_1}{\mu_1} \tag{30a}$$

$$w_2 = \frac{\beta_1}{\alpha_1 + \mu_1} w_6 \tag{30b}$$

$$w_3 = \frac{\alpha_1\ \beta_1}{(\alpha_1 + \mu_1)(\alpha_1 + \gamma_1 + \mu_1)} w_6 \tag{30c}$$

$$w_4 = \frac{\alpha_1 \gamma_1 \beta_1}{\mu_1\ (\alpha_1 + \mu_1)(\alpha_1 + \gamma_1 + \mu_1)} w_6 \tag{30d}$$

$$w_5 = \frac{\alpha_1 J_1 \gamma_1 \beta_1}{\mu_1\ (\alpha_1 + \mu_1)(\alpha_1 + \gamma_1 + \mu_1)(\pi_m + \mu_2)} w_6 \tag{30e}$$

$$w_6 = w_6 \tag{30f}$$

Further, $J_{\beta_1^*}$ has a left eigenvector$v = [v_1, v_2, v_3, v_4, v_5, v_6]$, where,

$$v_1 = 0, v_2 = \frac{\alpha_1}{\alpha_1 + \mu_1} v_3,\ v_3 = v_3, v_4 = v_4,\ v_5 = 0,$$

$$v_6 = -\frac{\alpha_1 \beta_1}{(\alpha_1 + \mu_1)(\pi_m + \mu_2)} v_3. \tag{31}$$

Computation of a and$b$[23]:

After some tedious manipulations it can be shown that

$$a = 2\ v_3\ \beta_1 (\tau w_6 + w_4)\{w_1 + w_2(1 - \varepsilon)\},$$

$$b = \frac{\Lambda v_3 (\tau w_6 + w_4)\{\mu + \rho(1 - \varepsilon)\}}{\mu(\mu + \rho)} \tag{32}$$

Thus, it follows from Theorem 4.1 of Castillo-Chavez & Song[24] that the LSD model (1) undergoes backward bifurcation at $R_0 = 1$ whenever $a > 0$and$b > 0$. The graphical representation of the backward bifurcation has been provided in Fig. 2.

Parameter values are used as $\mu_1 = 0.001$, $\mu_2 = 0.075$, $\Lambda_1 = 20$, $\Lambda_2 = 20,000$, $\beta_2 = 0.1$, $\alpha_1 = 0.4$, $\gamma_1 = 0.01$, $\sigma_1 = 0.1$, $\pi_M = 0.02$. From this figure, we can witness the co-existence of both the DFE and EEP when the basic reproduction number(R_0)is less than one. This implies that R_0less than one is not sufficient to eradicate the disease from the community.

Theorem 4: The endemic equilibrium point (EEP) is globally asymptotically stable (GAS) if$R_0 > 1$.

Proof: Let us consider the following Lyapunov function, L

$$L(t) = \frac{1}{2}(S_C - S_C^*)^2 + \frac{1}{2}(E_C - E_C^*)^2 + \frac{1}{2}(I_C - I_C^*)^2 + \frac{1}{2}(R_C - R_C^*)^2 + \frac{1}{2}(S_M - S_M^*)^2 + \frac{1}{2}(I_M - I_M^*)^2 \tag{33}$$

Differentiating Eq. (33) with respect to t, we get,

$$\frac{dL}{dt} = (S_C - S_C^*)\frac{dS_C}{dt} + (E_C - E_C^*)\frac{dE_C}{dt} + (I_C - I_C^*)\frac{dI_C}{dt} + (R_C - R_C^*)\frac{dR_C}{dt} + (S_M - S_M^*)\frac{dS_M}{dt} + (I_M - I_M^*)\frac{dI_M}{dt} \tag{34}$$

Let us consider the following equations,

$$\frac{dS_C}{dt} = \Lambda_1 - \frac{\beta_1}{N_C} S_C I_M - \mu_1 S_C \tag{35a}$$

At the equilibrium, we have

$$0 = \Lambda_1 - \frac{\beta_1}{N_C} S_C^* I_M^* - \mu_1 S_C^* \tag{35b}$$

And subtracting Eq. (35b) from Eq. (35a), we get

$$\frac{dS_C}{dt} = -\frac{\beta_1}{N_C}(\ S_C I_M - S_C^* I_M^*) - \mu_1 (S_C - S_C^*) \tag{36}$$

For simplicity, let us consider the first term of the right side of Eq. (34) and apply Eq. (36):

$$(S_C - S_C^*)\frac{dS_C}{dt} = (S_C - S_C^*)\left[-\frac{\beta_1}{N_C}(\ S_C I_M - S_C^* I_M^*) - \mu_1 (S_C - S_C^*)\right] \tag{37}$$

Let us expand the product term $(\ S_C I_M - S_C^* I_M^*)$ as:

$$(\ S_C I_M - S_C^* I_M^*) = (S_C - S_C^*) I_M + S_C^* (I_M - I_M^*) \tag{38a}$$

$$\Rightarrow (S_C - S_C^*)(\ S_C I_M - S_C^* I_M^*) = (S_C - S_C^*)^2 I_M + S_C^* (S_C - S_C^*)(I_M - I_M^*) \tag{38b}$$

Let us expand the part of second term of Eq. (38) by using Cauchy–Schwarz inequality and we get

$$|(S_C - S_C^*)(I_M - I_M^*)| \le |S_C - S_C^*|\ |I_M - I_M^*| \tag{39}$$

Now we will use Young's Inequality to simplify the LHS of Eq. (39). Therefore, we get

$$|(S_C - S_C^*)(I_M - I_M^*)| \le \frac{(S_C - S_C^*)^2}{2\varepsilon} + \frac{\varepsilon}{2}(I_M - I_M^*)^2,\ \varepsilon > 0 \tag{40}$$

It follows that

$$|S_C^*(S_C - S_C^*)(I_M - I_M^*)| \le |S_C^*|\left[\frac{(S_C - S_C^*)^2}{2\varepsilon} + \frac{\varepsilon}{2}(I_M - I_M^*)^2\right],\ \varepsilon > 0 \tag{41}$$

Now from the second term of the RHS of Eq. (38b):

$$S_C^*(S_C - S_C^*)(I_M - I_M^*) \le |S_C^*(S_C - S_C^*)(I_M - I_M^*)|$$

$$\Rightarrow S_C^*(S_C - S_C^*)(I_M - I_M^*) \le |S_C^*|\left[\frac{(S_C - S_C^*)^2}{2\varepsilon} + \frac{\varepsilon}{2}(I_M - I_M^*)^2\right] \tag{42}$$

Therefore, Eq. (38b) becomes

$$(S_C - S_C^*)(\ S_C I_M - S_C^* I_M^*) \le (S_C - S_C^*)^2 |I_M| + |S_C^*|\left[\frac{(S_C - S_C^*)^2}{2\varepsilon} + \frac{\varepsilon}{2}(I_M - I_M^*)^2\right] \tag{43}$$

From Eq. (37), we get

$$\left(S_C - S_C^*\right)\left[-\frac{\beta_1}{N_C}\left(S_C I_M - S_C^* I_M^*\right) - \mu_1\left(S_C - S_C^*\right)\right]$$
$$= -\frac{\beta_1}{N_C}\left(S_C - S_C^*\right)\left(S_C I_M - S_C^* I_M^*\right) - \mu_1\left(S_C - S_C^*\right)^2 \tag{44}$$

It follows that

$$\left(S_C - S_C^*\right)\frac{dS_C}{dt} \le -\frac{\beta_1}{N_C}\left\{\left(S_C - S_C^*\right)^2 |I_M| + |S_C^*|\left[\frac{\left(S_C - S_C^*\right)^2}{2\varepsilon} + \frac{\varepsilon}{2}\left(I_M - I_M^*\right)^2\right]\right\} \tag{45}$$

Which implies that

$$\left(S_C - S_C^*\right)\frac{dS_C}{dt} \le -\frac{\beta_1}{N_C}\left(S_C - S_C^*\right)^2 |I_M| - \frac{\beta_1}{N_C}|S_C^*|\left[\frac{\left(S_C - S_C^*\right)^2}{2\varepsilon} + \frac{\varepsilon}{2}\left(I_M - I_M^*\right)^2\right] \tag{46}$$

Hence

$$\left(S_C - S_C^*\right)\frac{dS_C}{dt} \le -A\left(S_C - S_C^*\right)^2 - B\left(I_M - I_M^*\right)^2 \tag{47}$$

where $A = \frac{\beta_1}{N_C}\left(|I_M| + \frac{|S_C^*|}{2\varepsilon}\right) > 0$, $B = \frac{\beta_1 |S_C^*|\varepsilon}{2N_C} > 0$ are constants depending on bounds of S_c^* andI_m.

Similar approaches can be used to get rid of the cross terms for the other terms in Eq. 34. Therefore, we have shown that $dL/dt = 0$ only at the endemic equilibrium point and is negative at all other points. Thus, we have demonstrated (utilizing the LaSalle invariance principle) that the endemic equilibrium point is globally asymptotically stable.

Sensitivity Analysis:

This section explores into the numerical simulation of the LSD model. To address the system of Eqs. (1), we utilize the Euler scheme for solving and implementation, followed by graphical presentation of the results. The time unit is expressed in days, with corresponding numerical values assigned to the model parameters, outlined in Table 2.

The basic reproduction number i.e.,

$$R_0 = \frac{1}{(\mu_2 + \pi_M)}\sqrt{\frac{\alpha_1\beta_1\beta_2\Lambda_2\mu_1}{\Lambda_1(\alpha_1 + \mu_1)(\gamma_1 + \sigma_1 + \mu_1)}} \tag{48}$$

plays a pivotal role while this is being used to analyze sensitivity. This study will inform us about the significance of the parameters spreading the disease in society. Considering the inaccuracy of the data collection and parameter assumptions, sensitivity analysis is a reliable mechanism to estimate the model's robustness and influence on parameter values. Moreover, sensitivity indices analyze social changes while the parameter modified as presented in Eq. (49). Here we have the following parameters μ_1,μ_2,Λ_1,Λ_2,β_1,β_2,α_1,γ_1,$\sigma_1$and π_M.

In our investigation, we examined the sensitivity of each parameter contributing to R_0,[22] as outlined in Table 3 and illustrated in Fig. 3, where The parameters analyzed include recruitment rates (Λ_1,Λ_2), transmission rates (β_1,β_2), natural and temperature-dependent mortality rates (μ_1,μ_2,andπ_M), disease progression and recovery rates (α_1,γ_1), and disease-induced mortality rate (σ_1). The results, presented in a bar chart, highlight the relative influence of each parameter on the model outcomes. Among these parameters, some exhibit negative values, suggesting a negative influence on R_0, while others have a positive impact on disease transmission dynamics.

The results presented in Fig. 3 and Table 3 highlight that the temperature-dependent death rate of flies (π_M) has the highest negative sensitivity index (-0.995), indicating that temperature fluctuations significantly impact disease persistence. This suggests that environmental factors, particularly temperature variations, play a crucial role in controlling fly populations and, consequently, disease transmission. Additionally, the recruitment rates of cows and flies (Λ_1,Λ_2) and the transmission rates from flies to cows(β_1) and cows to flies (β_2) exhibit a strong positive influence on R_0 (0.5 each), reinforcing that increased host and vector populations and increased transmission rate enhance disease spread. Conversely, higher recovery rates ($\gamma_1 = -0.235$), higher temperature-induced death rate of flies(π_M), and disease-induced mortality ($\sigma_1 = -0.235$) reduce R_0, highlighting the role of medical interventions in limiting outbreaks. While the natural death rate of cows (μ_1) has a moderate negative effect (-0.471), fly mortality (μ_2) has minimal influence (-0.005), indicating that disease control efforts should prioritize factors beyond natural mortality.

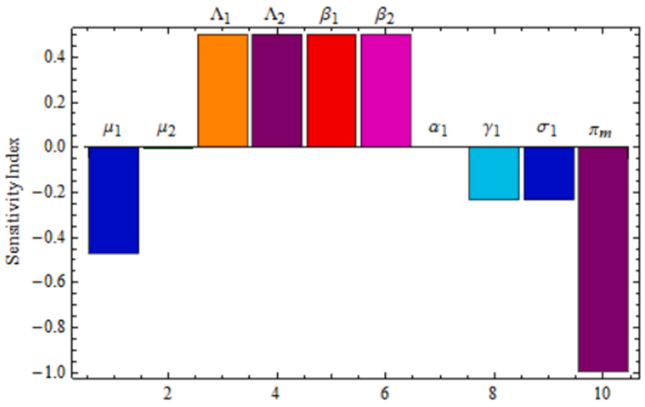

Fig. 3. Representation of parameters as a bar diagram.

$$\left.\begin{aligned}
\Gamma_{R_0}^{\sigma} &= \frac{\sigma}{R_0}\cdot\frac{\partial R_0}{\partial \sigma}\\
\Gamma_{R_0}^{\mu_1} &= \frac{\mu_1}{R_0}\cdot\frac{\partial R_0}{\partial \mu_1} = -\frac{\alpha_1\gamma_1 + \alpha_1\sigma_1 - \mu_1^2}{2\mu_1}\\
\Gamma_{R_0}^{\mu_2} &= \frac{\mu_2}{R_0}\cdot\frac{\partial R_0}{\partial \mu_2} = -\frac{\mu_2}{(\mu_2 + \pi M)}\\
\Gamma_{R_0}^{\wedge_1} &= \frac{\wedge_1}{R_0}\cdot\frac{\partial R_0}{\partial \wedge_1} = \frac{1}{2}\\
\Gamma_{R_0}^{\wedge_2} &= \frac{\wedge_2}{R_0}\cdot\frac{\partial R_0}{\partial \wedge} = \frac{1}{2}\\
\Gamma_{R_0}^{\beta_1} &= \frac{\beta_1}{R_0}\cdot\frac{\partial R_0}{\partial \beta_1} = \frac{1}{2}\\
\Gamma_{R_0}^{\beta_1} &= \frac{\beta_1}{R_0}\cdot\frac{\partial R_0}{\partial \beta_2} = \frac{1}{2}\\
\Gamma_{R_0}^{\alpha_1} &= \frac{\alpha_1}{R_0}\cdot\frac{\partial R_0}{\partial \alpha} = 1\frac{\mu_1}{2\alpha_1\sqrt{\alpha_1 + \mu_1}}\\
\Gamma_{R_0}^{\gamma_1} &= \frac{\gamma_1}{R_0}\cdot\frac{\partial R_0}{\partial \gamma_1} = -\frac{\gamma 1}{2(\gamma_1 + \sigma_1 + \mu_1)}\\
\Gamma_{R_0}^{\sigma_1} &= \frac{\sigma_1}{R_0}\cdot\frac{\partial R_0}{\partial \sigma_1} = -\frac{\sigma_1}{2(\gamma_1 + \sigma_1 + \mu_1)}\\
\Gamma_{R_0}^{\pi_M} &= \frac{\pi_M}{R_0}\cdot\frac{\partial R_0}{\partial \pi_M} = -\frac{\pi_M}{(\mu_2 + \pi_M)}
\end{aligned}\right\} \tag{49}$$

Table 3
Initial values for different compartments and different parameter values.

	$\Gamma_{R_0}^{\mu_2}$	$\Gamma_{R_0}^{\Lambda_1}$	$\Gamma_{R_0}^{\Lambda_2}$	$\Gamma_{R_0}^{\beta_1}$	$\Gamma_{R_0}^{\beta_2}$	$\Gamma_{R_0}^{\alpha_1}$	$\Gamma_{R_0}^{\gamma_1}$	$\Gamma_{R_0}^{\sigma_1}$	$\Gamma_{R_0}^{\pi_M}$
-0.471	-0.005	0.5	0.5	0.5	0.5	-0.0011	-0.235	-0.235	-0.995

We can use that above calculation to get the analytical values of the parameters from the following Table 3:

While their sensitivity indices are comparatively lower, their impact is evident in numerical simulations, as illustrated in Fig. 4a and Fig. 4b. Notably, γ_1,μ_1 and σ_1 exert the greatest influence on the solution, with K_2 demonstrating a notably significant effect, far surpassing other parameters. The observation from Fig. 3 underscores the profound impact ofγ_1,$\mu_1$andσ_1, suggesting that controlling these parameters, particularly K_2, offers a potentially efficient strategy for disease management. The sensitivity of the solution to K_2 implies that even marginal adjustments in this parameter yield substantial changes in the outcome, emphasizing its pivotal role in disease control strategies.

To validate our numerical findings regarding the effects of parameter adjustments, a sensitivity analysis, as depicted in Fig. 3, has been conducted. This analysis reinforces our conclusion that alterations in recruitment and transmission rates exert remarkable influence on model outcomes. Fig. 4. illustrates the effect of recruitment rates of flies, the transmission rates from infected cows to flies, from infected flies to cows, and from exposed to infected cows. All of them have negative effect on the cow population. Thus, disease related complexity increases when values of these parameters increase. This figure also presents the effect of natural death rate of flies, temperature related death rate of flies and recovery rate of cows. These parameters have positive impact on the disease dynamics. Hence, a decrease in the disease-related complexity is observed when these parameter values increase.

Fig. 4a. shows that infected cow population increase due to an increase in flies population(Λ_2). So, flies population should be controlled by closely monitoring larval and adult flies number. If this number increases remarkably, necessary steps must be taken to control their number. From this figure it is also clear that transmission rate should be minimized to control the disease outbreak as an increase in the transmission rate($\beta_1$andβ_2)increase the number infected cows. This can be done by isolating the infected cows. Our research findings confirm the practical validity of the decrease in the infected population of cows due to an increase in recovery rate(γ_1) as shown in Fig. 4b. Additionally, this figure illustrates that increase in natural death rate(μ_2)and temperature-dependent death rate(π_m) of flies can slow down the disease progression. Moreover, this figure depicts that if the incubation rate$1/\alpha_1$decreases, that is, if(α_1)increases, the disease spreads too fast.

While an increase in temperature-dependent mortality rates of mosquitoes might reduce their population, flies may thrive under the same conditions.

LSD management strategies:

Countries like Russia, Israel, Namibia, India, Bangladesh, China, Turkey, Saudi Arabia, Iran, and Greece have experienced severe outbreaks of Lumpy Skin Disease (LSD) in recent years. In response, many of these countries implemented large-scale vaccination programs to control the disease's spread among cattle. Additionally, strict animal movement restrictions and quarantine measures were put in place to contain the outbreaks. Insecticide spraying has also been used to control the vector populations responsible for transmission, while public awareness programs have been promoted to educate farmers about prevention and early detection. Early identification of LSD cases is crucial, as it enables more effective containment of outbreaks and reduces the risk of further spread.[25] Also, Table 4 presents the name of some countries where vaccination is used to control the LSD.

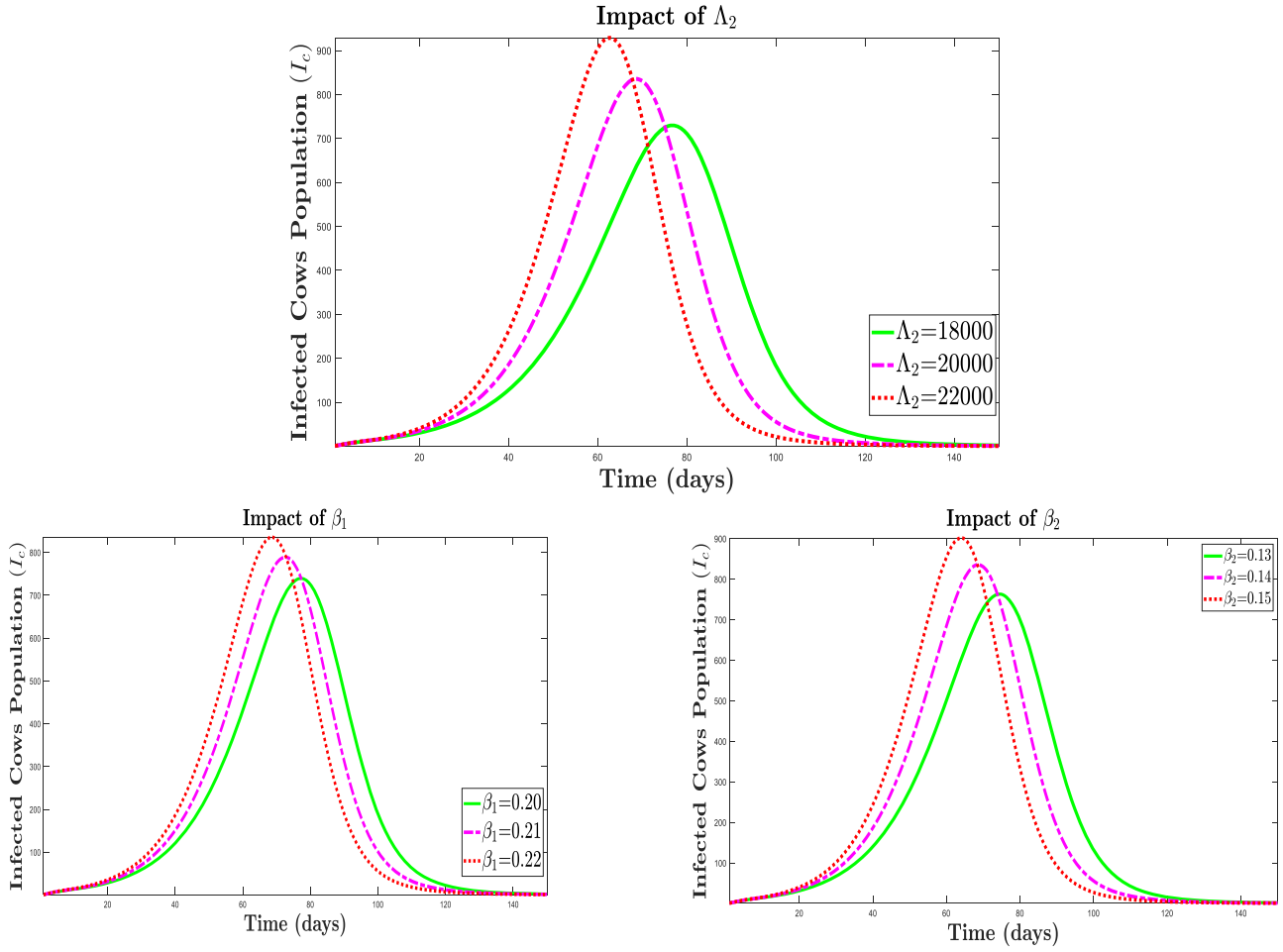

Fig. 4a. Effect of different parameters on infected cow's population.

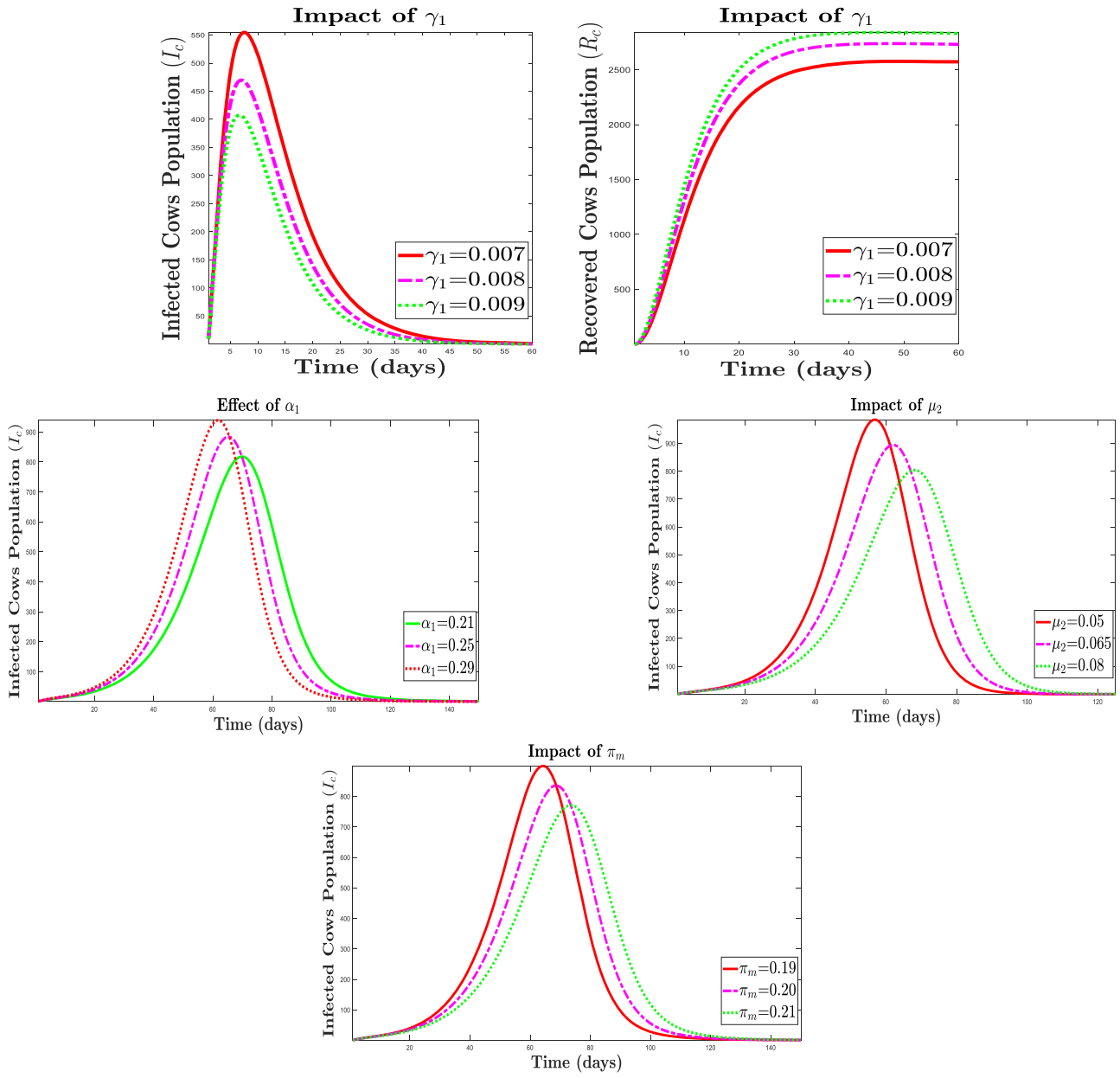

Figure 4b. Effect of different parameters on infected cow's population.

Table 4
Name of the countries and name of the vaccines for LSD diseases.[25].

Name of the country	Vaccine used
South Africa	Lumpy Skin Disease, Vaccine for Cattle Lumpyvax™
Morocco	Bovivax-LSD™
Jordan	LumpyShield-N™
Egypt	MEVAC LSD
Ethiopia	Lumpy Skin Disease, Vaccine
Kenya	Lumpivax™
Turkey	Penpox-M™, Live SPPV, Poxvac™, Lumpyvac™, Poxdoll™
Russia	Sheep Pox Cultyral, Dry™

5. Conclusion

In this study, we developed an SEIR (cow)-SI (flies) model aimed at investigating the dynamics of LSD transmission. Our initial focus involved theoretical analysis, and we established key factors of the model. Specifically, we demonstrated both local and global stability at equilibrium points. Additionally, we conducted sensitivity analysis to evaluate the influence of various model parameters onR_0, identifying those parameters most crucial for effective disease management. Some of the key findings are:

- Effective prevention techniques by farmers delay rapid disease spread.
- Low infection rate reduces transmission rates insignificant.
- Adjustments in recruitment rate and transmission rates affect model outcomes.
- Recovered cow populations may become re-infected with different LSD strains due to contact rates, clustering, or inadequate hygiene among farmers.
- Temperature-dependent death rate and natural death rate of vectors have positive impact on decreasing infected cow population.

6. Limitations

- Our study does not incorporate optimal control analysis,[26,27] which could provide insights into cost-effective strategies for managing LSD.
- The model assumes a direct transmission pathway between cows and flies but does not consider complex ecological interactions, such as fly movement patterns, seasonal variations in fly populations, or cow-to-cow transmission.
- The model accounts for a temperature-dependent fly mortality rate but does not include other environmental factors, such as humidity, precipitation, or habitat availability, which could influence fly survival and disease spread.

Ethical approval and consent to participate

Not applicable, as no human participants were involved.

Availability of data and materials

All data are available in the manuscript.

Financial support and sponsorship

None.

AI Declaration

The authors used AI-assisted technology (ChatGPT-3.5) for language editing and grammar checking.

CRediT authorship contribution statement

Goutam Saha: Conceptualization, Supervision, Methodology, Software, Writing – original draft, Writing – review & editing. **Pabel Shahrear:** Methodology, Investigation, Writing – original draft, Writing – review & editing. **Abrar Faiyaz:** Methodology, Investigation, Writing – original draft, Writing – review & editing. **Amit Kumar Saha:** Methodology, Software, Visualization, Investigation, Writing – review & editing.

Declaration of competing interest

The authors declare that they have no known competing financial interests or personal relationships that could have appeared to influence the work reported in this paper.

Acknowledgement

The authors declare that there are no acknowledgements for this study.

Data availability

No data was used for the research described in the article.

References

1. Talukdar F, Fakir A, Hasan Z, Osmani TMG, Choudhury GA, Budhay S, Sadekuzzaman M, Brum E, Bhowmic HR, Noorjahan B. Identification of Lumpy skin disease (LSD): First-time in Bangladesh during the investigation of unknown skin disease of cattle. *Int J Infect Dis*. 2020;101:360–361. https://doi.org/10.1016/j.ijid.2020.09.946.
2. Molla W, Frankena K, De Jong MCM. Transmission dynamics of lumpy skin disease in Ethiopia. *Epidemiol Infect*. 2017;145(13):2856–2863. https://doi.org/10.1017/S0950268817001637.
3. Ardestani EG, Mokhtari A. Modeling the lumpy skin disease risk probability in central Zagros Mountains of Iran. *Prev Vet Med*. 2020;176, 104887. https://doi.org/10.1016/j.prevetmed.2020.104887.
4. Sarkar S, Meher MM, Parvez MMM, Akther M. Occurrences of lumpy skin disease (LSD) in cattle in Dinajpur Sadar of Bangladesh. *Res Agric Livestock Fisher*. 2020;7(3):445–455. https://doi.org/10.3329/ralf.v7i3.51364.
5. Hasib FMY, Islam MS, Das T, Rana EA, Uddin MH, Bayzid M, Nath C, Hossain MA, Masuduzzaman M, Das S, Alim MA. Lumpy skin disease outbreak in cattle population of Chattogram, Bangladesh. *Vet Med Sci*. 2021;7(5):1616–1624. https://doi.org/10.1002/vms3.524.
6. Haque MH, Roy RK, Yeasmin F, Fakhruzzaman M, Yeasmin T, Sazib MdRI, Uddin MdN, Sarker S. Prevalence and management practices of lumpy skin disease (LSD) in cattle at Natore District of Bangladesh. *Eur J Agric Food Sci*. 2021;3(6):76–81. https://doi.org/10.24018/ejfood.2021.3.6.420.
7. Khalil MdI, Sarker MFR, Hasib FMY, Chowdhury S, Eleroğlu H. Outbreak investigation of lumpy skin disease in dairy farms at Barishal, Bangladesh. *Turkish J Agric Food Sci Technol*. 2021;9(1):205–209. https://doi.org/10.24925/turjaf.v9i1.205-209.3827.
8. Pory FS, Lasker RM, Islam MN, Siddiqui MSI. Prevalence of lumpy skin disease at district veterinary hospital in Sylhet district of Bangladesh. *Int J Res Innov Appl Sci*. 2021;6(10):111–115.
9. Chouhan CS, Parvin MstS, Ali MdY, Sadekuzzaman M, Chowdhury MdGA, Ehsan MdA, Islam MdT. Epidemiology and economic impact of lumpy skin disease of cattle in Mymensingh and Gaibandha districts of Bangladesh. *Transbound Emerg Dis*. 2022;69(6):3405–3418. https://doi.org/10.1111/tbed.14697.
10. Issimov A, Kushaliyev K, Abekeshev N, Molla W, Rametov N, Bayantassova S, Zhanabayev A, Paritova A, Shalmenov M, Ussenbayev A, Kemeshov Z, Baikadamova G, White P. Risk factors associated with lumpy skin disease in cattle in West Kazakhstan. *Prev Vet Med*. 2022;207, 105660. https://doi.org/10.1016/j.prevetmed.2022.105660.
11. Afshari Safavi E. Assessing machine learning techniques in forecasting lumpy skin disease occurrence based on meteorological and geospatial features. *Trop Anim Health Prod*. 2022;54(1):55. https://doi.org/10.1007/s11250-022-03073-2.
12. Uddin MA, Islam MdA, Rahman AKMA, Rahman MM, Khasruzzaman AKM, Ward MP, Hossain MT. Epidemiological investigation of lumpy skin disease outbreaks in Bangladeshi cattle during 2019–2020. *Transbound Emerg Dis*. 2022;69(6):3397–3404. https://doi.org/10.1111/tbed.14696.
13. Alfwzan WF, DarAssi MH, Allehiany FM, Khan MA, Alshahrani MY, Tag-eldin EM. A novel mathematical study to understand the Lumpy skin disease (LSD) using modified parameterized approach. *Result Phys*. 2023;51, 106626. https://doi.org/10.1016/j.rinp.2023.106626.
14. Butt AIK, Aftab H, Imran M, Ismaeel T. Mathematical study of lumpy skin disease with optimal control analysis through vaccination. *Alex Eng J*. 2023;72:247–259. https://doi.org/10.1016/j.aej.2023.03.073.
15. Moonchai S, Himakalasa A, Rojsiraphisal T, Arjkumpa O, Panyasomboonying P, Kuatako N, Buamithup N, Punyapornwithaya V. Modelling epidemic growth models for lumpy skin disease cases in Thailand using nationwide outbreak data, 2021–2022. *Inf Dis Modell*. 2023;8(1):282–293. https://doi.org/10.1016/j.idm.2023.02.004.
16. Sthitmatee N, Tankaew P, Modethed W, Rittipornlertrak A, Muenthaisong A, Apinda N, Koonyosying P, Nambooppha B, Chomjit P, Sangkakam K, Singhla T, Vinitchaikul P, Boonsri K, Pringproa K, Punyapornwithaya V, Kreausukon K. Development of in-house ELISA for detection of antibodies against lumpy skin disease virus in cattle and assessment of its performance using a Bayesian approach. *Heliyon*. 2023;9(2), e13499. https://doi.org/10.1016/j.heliyon.2023.e13499.
17. Sayed A, Hossain M, Akter S, Rashid M. Demographic factors influencing Lumpy Skin Disease (LSD) prevalence at Barishal district in Bangladesh: A retrospective study. *J Bangladesh Agric Univ*. 2023;1. https://doi.org/10.5455/JBAU.135650.
18. Elsonbaty A, Alharbi M, El-Mesady A, Adel W. Dynamical analysis of a novel discrete fractional lumpy skin disease model. *Partial Differ Equ Appl Math: A Spin-off Appl Math Lett*. 2024;9, 100604. https://doi.org/10.1016/j.padiff.2023.100604.
19. El-Mesady A, Elsadany AA, Mahdy AMS, Elsonbaty A. Nonlinear dynamics and optimal control strategies of a novel fractional-order lumpy skin disease model. *J Comput Sci*. 2024;79, 102286. https://doi.org/10.1016/j.jocs.2024.102286.
20. Adel W, Srivastava HM, Izadi M, Elsonbaty A, El-Mesady A. Dynamics and numerical analysis of a fractional-order toxoplasmosis model incorporating human and cat populations. *Bound Value Probl*. 2024;2024(1):152. https://doi.org/10.1186/s13661-024-01965-w. –32.
21. Hanif A, Butt AIK, Ahmad S, Din RU, Inc M. A new fuzzy fractional order model of transmission of Covid-19 with quarantine class. *Eur Phys J Plus*. 2021;136(11):1179. https://doi.org/10.1140/epjp/s13360-021-02178-1.
22. Shahrear P, Rahman SMS, Nahid MMH. Prediction and mathematical analysis of the outbreak of coronavirus (COVID-19) in Bangladesh. *ResultAppl Math*. 2021;10, 100145. https://doi.org/10.1016/j.rinam.2021.100145.
23. Carr J. *Applications of Centre Manifold Theory*. 35. Springer; 2012, 1982 edition.
24. Castillo-Chavez C, Song B. Dynamical models of tuberculosis and their applications. *Math Biosci Eng*. 2004;1(2):361–404. https://doi.org/10.3934/mbe.2004.1.361.
25. Tuppurainen E, Dietze K, Wolff J, Bergmann H, Beltran-Alcrudo D, Fahrion A, Lamien CE, Busch F, Sauter-Louis C, Conraths FJ, De Clercq K, Hoffmann B, Knauf S. Review: Vaccines and vaccination against lumpy skin disease. *Vaccines (Basel)*. 2021;9(10):1136. https://doi.org/10.3390/vaccines9101136.
26. Berhe HW, Gebremeskel AA, Melese ZT, Al-arydah M, Gebremichael AA. Modeling and global stability analysis of COVID-19 dynamics with optimal control and cost-

effectiveness analysis. *Partial Differ Equ Appl Math: A Spin-off Appl Math Lett*. 2024; 11, 100843-. https://doi.org/10.1016/j.padiff.2024.100843.
27. Forrest O, Al-arydah M. Optimal control strategies for infectious diseases with consideration of behavioral dynamics. *Math Method Appl Sci*. 2025;48(2): 1362–1380. https://doi.org/10.1002/mma.10388.
28. Islam MS, Shahrear P, Saha G, Ataullha M, Rahman MS. Mathematical analysis and prediction of future outbreak of dengue on time-varying contact rate using machine learning approach. *Comput Biol Med*. 2024;178, 108707. https://doi.org/10.1016/j.compbiomed.2024.108707.